Supplementary Materials

1. **Supplementary Methods section**
2. **Suppementary Table: Table S1**
3. **Supplementary Figures: Figures S1, S2 and S3**

1. Supplementary Methods.

Participant Inclusion Criteria

The inclusion criteria for cognitively normal LLD subjects included persons with major depression (n = 23), according to the SCID.[54] All participants had a GDS score of 10 or above, PSMS ≤ 6 and IADL ≤ 9,[55] score above the education-adjusted cutoff on the LMII-DR (Delayed recall score > 8 for 16 or more years of education or score > 4 for 8–15 years of education).[56]

Amnestic mild cognitive impairment (aMCI) (n = 18) was operationally defined according to the established criteria: (1) subjective report of cognitive decline; (2) objective cognitive impairment that includes scoring 1.5 SD below on memory measures; (3) intact ADLs and relatively preserved IADLs; and (4) no dementia. For meeting criteria for objective cognitive impairment, participants had to score below the education-adjusted cutoff on the LMII-DR (i.e., ≤ 8 for 16 or more years of education, and ≤ 4 for 8-15 years of education), and score below 1.5 SD below the mean on one or more subscales (one of the impairments had to be memory) of the Repeatable Battery for the Assessment of Neuropsychological Status (RBANS),[57] Behavioral Dyscontrol scale or the Boston Naming Test.

All participants diagnosed with aMCI who subsequently met criteria for clinically significant depression, according to SCID standards (major depression: n = 12; dysthymic disorder: n = 1), were included in the comorbid LLD and aMCI (aMCI-LLD) group (total n = 13).

The eligibility criteria for control subjects (n = 25) were similar to that used for the LLD-only group except these subjects could not meet criteria for depression.

Graph Theoretical Measurements

Small-world properties. To examine the graph theoretical properties of the 264 region of interest (ROI) brain functional networks, each individual cross-correlation matrix was first converted to an undirected and unweighted binary network (*G, i.e., graph*). The binary matrix was then thresholded over a range of thresholds using network cost (detail is shown below). In a given network, the *nodes* represent the brain regions, and *edges* represent the connections between pairs of brain regions. Like many naturally occurring networks in the economic, social, and biological systems, the human brain is a complex network that behaves like a small-world network.[58] Watts and Strogatz first proposed that the shortest path length (*L*: shortest distance between a pair of nodes) and clustering coefficient (*C*: number of edges passing through a node) could be used to quantify a network's small-world properties.[16] A network's small-worldness (σ) can then be characterized as the ratio between absolute clustering coefficient ($\gamma = C_{real}/C_{random}$) and absolute path length ($\lambda = L_{real}/L_{random}$). A small-world-like network will have $\gamma > 1$, and $\lambda \approx 1$.[16, 59]

Network cost. A network property, *cost*, was utilized to threshold against the topological measurements because of its close association with information transfer efficiencies in a given network.[17, 60, 61]

$$Cost = \frac{2K}{N(N-1)}$$

Where *K* and *N* are the total number of edges and nodes in a network. Higher cost threshold will yield sparser network connectivity and lower cost threshold will yield denser connections. A range of *cost* ($0.05 < cost < 0.5$) was selected to ensure that all individual subnetworks sustained a complete graph as the graph started becoming fragmented as the cost threshold became lower.[17, 60, 62]

Network Efficiencies. More recently, Achard and Bullmore showed that human brain functional network behaved like an economical small-world network, which supports efficient parallel information transfer at a relatively low cost.[17] Furthermore, they demonstrated that aging altered the brain's functional network economic efficiencies. We employed network efficiency measures to investigate the abnormal changes among the brain networks of cognitively normal (CN), LLD, aMCI, and aMCI-LLD participants. The global efficiency (E_{Global}), which primarily measures the information integration of the entire network, is defined as the inverse harmonic mean of the shortest path length.[15, 63]

$$E_{Global} = \frac{1}{N(N-1)} \sum_{i \neq j \in G} \frac{1}{L_{ij}}$$

Where L_{ij} is the shortest path length between node *i* and node *j.* The local efficiency (E_{Local}), which measures the information segregation of the network, is defined as the average of all subnetworks in the network.[15, 63]

$$E_{Local} = \frac{1}{N_{G_i}(N_{G_i}-1)} \sum_{j,k \in G_i} \frac{1}{L_{j,k}}$$

The nodal efficiency (E_{Nodal}), which measures the regional parallel information transfer between a node and the rest of the network, is defined as the harmonic mean of the shortest path length between node *i* and all other nodes in the network.[15, 17]

$$E_{Nodal,i} = \frac{1}{N-1} \sum_{j \in G} \frac{1}{L_{i,j}}$$

Betweenness centrality. We also measured the betweenness centrality, which is defined as the number of shortest paths connecting a given node, to characterize the brain functional network hub nodes.[15, 64]

$$B_i = \sum_{j \neq i, k \neq i} \frac{\eta_{jk}(i)}{\eta_{jk}}$$

Where η_{jk} is the total number of shortest paths between node *j* and *k* and $\eta_{jk}(i)$ is the number of shortest paths that pass through node *i*.

Modularity. The human brain network is a combination of densely intraconnected modules (i.e. subnetworks) that are sparsely interconnected. To characterize brain functional network modular structure, we estimated the modularity (*Q*).

$$Q = \frac{1}{l} \sum_{i,j \in N} (a_{ij} - \frac{\kappa_i \kappa_j}{l}) \delta_{m_i, m_j}$$

Where *l* is the number of connected edges, a_{ij} is the connection status (1 if a link exist between *i* and *j* and 0 otherwise), κ is the degree (number of connected links) of a node, m_i is the module containing node *i, and* $\delta = 1$ if $m_i = m_j$ and 0 otherwise.[15, 18]

All of the graph theoretical properties and efficiency measurements were estimated using in-house written Matlab programs and Matlab functions provided by the Brain Connectivity Toolbox (www.brain-connectivity-toolbox.net).[15]

References

1. Alexopoulos GS. Depression in the elderly. *Lancet*. 2005; **365**: 1961-70.
2. Steffens DC, Otey E, Alexopoulos GS, et al. Perspectives on depression, mild cognitive impairment, and cognitive decline. *Archives of general psychiatry*. 2006; **63**: 130-8.
3. Aizenstein HJ, Butters MA, Figurski JL, et al. Prefrontal and striatal activation during sequence learning in geriatric depression. *Biological psychiatry*. 2005; **58**: 290-6.
4. Dickerson BC, Sperling RA. Large-scale functional brain network abnormalities in Alzheimer's disease: insights from functional neuroimaging. *Behav Neurol*. 2009; **21**: 63-75.
5. Tadayonnejad R, Ajilore O. Brain network dysfunction in late-life depression: a literature review. *Journal of geriatric psychiatry and neurology*. 2014; **27**: 5-12.
6. Biswal B, Yetkin FZ, Haughton VM, et al. Functional connectivity in the motor cortex of resting human brain using echo-planar MRI. *Magnetic resonance in medicine : official journal of the Society of Magnetic Resonance in Medicine / Society of Magnetic Resonance in Medicine*. 1995; **34**: 537-41.
7. Biswal BB, Mennes M, Zuo X-N, et al. Toward discovery science of human brain function. *Proceedings of the National Academy of Sciences of the United States of America*. 2010; **107**: 4734-9.
8. Kenny ER, O'Brien JT, Cousins DA, et al. Functional connectivity in late-life depression using resting-state functional magnetic resonance imaging. *The American journal of geriatric psychiatry : official journal of the American Association for Geriatric Psychiatry*. 2010; **18**: 643-51.
9. Andreescu C, Wu M, Butters MA, et al. The default mode network in late-life anxious depression. *The American journal of geriatric psychiatry : official journal of the American Association for Geriatric Psychiatry*. 2011; **19**: 980-3.
10. Alexopoulos GS, Hoptman MJ, Kanellopoulos D, et al. Functional connectivity in the cognitive control network and the default mode network in late-life depression. *Journal of affective disorders*. 2012; **139**: 56-65.
11. Xie C, Li W, Chen G, et al. Late-life depression, mild cognitive impairment and hippocampal functional network architecture. *NeuroImage Clinical*. 2013; **3**: 311-20.
12. Sheline YI, Raichle ME. Resting state functional connectivity in preclinical Alzheimer's disease. *Biological psychiatry*. 2013; **74**: 340-7.
13. Xie C, Bai F, Yu H, et al. Abnormal insula functional network is associated with episodic memory decline in amnestic mild cognitive impairment. *NeuroImage*. 2012; **63**: 320-7.
14. Bullmore E, Sporns O. Complex brain networks: graph theoretical analysis of structural and functional systems. *Nature reviews Neuroscience*. 2009; **10**: 186-98.
15. Rubinov M, Sporns O. Complex network measures of brain connectivity: uses and interpretations. *NeuroImage*. 2010; **52**: 1059-69.
16. Watts DJ, Strogatz SH. Collective dynamics of 'small-world' networks. *Nature*. 1998; **393**: 440-2.
17. Achard S, Bullmore E. Efficiency and cost of economical brain functional networks. *PLoS Comput Biol*. 2007; **3**: e17.
18. Newman ME. Modularity and community structure in networks. *Proceedings of the National Academy of Sciences of the United States of America*. 2006; **103**: 8577-82.
19. Achard S, Delon-Martin C, Vertes PE, et al. Hubs of brain functional networks are radically reorganized in comatose patients. *Proceedings of the National Academy of Sciences of the United States of America*. 2012; **109**: 20608-13.
20. Meunier D, Achard S, Morcom A, et al. Age-related changes in modular organization of human brain functional networks. *NeuroImage*. 2009; **44**: 715-23.
21. Bohr IJ, Kenny E, Blamire A, et al. Resting-state functional connectivity in late-life depression: higher global connectivity and more long distance connections. *Frontiers in psychiatry*. 2012; **3**: 116.

22. Lord A, Horn D, Breakspear M, et al. Changes in community structure of resting state functional connectivity in unipolar depression. *PloS one*. 2012; **7**: e41282.
23. Liu Z, Zhang Y, Yan H, et al. Altered topological patterns of brain networks in mild cognitive impairment and Alzheimer's disease: a resting-state fMRI study. *Psychiatry research*. 2012; **202**: 118-25.
24. Wang J, Zuo X, Dai Z, et al. Disrupted functional brain connectome in individuals at risk for Alzheimer's disease. *Biological psychiatry*. 2013; **73**: 472-81.
25. Brier MR, Thomas JB, Fagan AM, et al. Functional connectivity and graph theory in preclinical Alzheimer's disease. *Neurobiology of aging*. 2014; **35**: 757-68.
26. Lim HK, Jung WS, Aizenstein HJ. Aberrant topographical organization in gray matter structural network in late life depression: a graph theoretical analysis. *International psychogeriatrics / IPA*. 2013; **25**: 1929-40.
27. Ajilore O, Lamar M, Leow A, et al. Graph theory analysis of cortical-subcortical networks in late-life depression. *The American journal of geriatric psychiatry : official journal of the American Association for Geriatric Psychiatry*. 2014; **22**: 195-206.
28. Bai F, Shu N, Yuan Y, et al. Topologically Convergent and Divergent Structural Connectivity Patterns between Patients with Remitted Geriatric Depression and Amnestic Mild Cognitive Impairment. *The Journal of neuroscience : the official journal of the Society for Neuroscience*. 2012; **32**: 4307-18.
29. Ajilore O, Lamar M, Kumar A. Association of brain network efficiency with aging, depression, and cognition. *The American journal of geriatric psychiatry : official journal of the American Association for Geriatric Psychiatry*. 2014; **22**: 102-10.
30. Li W, Muftuler LT, Chen G, et al. Effects of the coexistence of late-life depression and mild cognitive impairment on white matter microstructure. *Journal of the neurological sciences*. 2014; **338**: 46-56.
31. Butters MA, Whyte EM, Nebes RD, et al. The nature and determinants of neuropsychological functioning in late-life depression. *Archives of general psychiatry*. 2004; **61**: 587-95.
32. Woodard JL, Seidenberg M, Nielson KA, et al. Semantic memory activation in amnestic mild cognitive impairment. *Brain : a journal of neurology*. 2009; **132**: 2068-78.
33. Debruyne H, Van Buggenhout M, Le Bastard N, et al. Is the geriatric depression scale a reliable screening tool for depressive symptoms in elderly patients with cognitive impairment? *International journal of geriatric psychiatry*. 2009; **24**: 556-62.
34. Van der Mussele S, Fransen E, Struyfs H, et al. Depression in Mild Cognitive Impairment is associated with Progression to Alzheimer's Disease: A Longitudinal Study. *J Alzheimers Dis*. 2014; **7**: 7.
35. Power JD, Cohen AL, Nelson SM, et al. Functional network organization of the human brain. *Neuron*. 2011; **72**: 665-78.
36. Strehl A, Ghosh J. Cluster ensembles---a knowledge reuse framework for combining multiple partitions. *The Journal of Machine Learning Research*. 2003; **3**: 583-617.
37. Benjamini Y, Hochberg Y. Controlling the False Discovery Rate: A Practical and Powerful Approach to Multiple Testing. *Journal of the Royal Statistical Society*. 1995; **57**: 289-300.
38. Zhang D, Raichle ME. Disease and the brain's dark energy. *Nature reviews Neurology*. 2010; **6**: 15-28.
39. Menon V, Uddin LQ. Saliency, switching, attention and control: a network model of insula function. *Brain structure & function*. 2010; **214**: 655-67.
40. Veer IM, Beckmann CF, van Tol MJ, et al. Whole brain resting-state analysis reveals decreased functional connectivity in major depression. *Frontiers in systems neuroscience*. 2010; **4**: 1-10.

41. Manoliu A, Meng C, Brandl F, et al. Insular dysfunction within the salience network is associated with severity of symptoms and aberrant inter-network connectivity in major depressive disorder. *Frontiers in human neuroscience*. 2013; **7**: 930.
42. Bracht T, Federspiel A, Schnell S, et al. Cortico-cortical white matter motor pathway microstructure is related to psychomotor retardation in major depressive disorder. *PloS one*. 2012; **7**: e52238.
43. Annweiler C, Beauchet O, Bartha R, et al. Motor cortex and gait in mild cognitive impairment: a magnetic resonance spectroscopy and volumetric imaging study. *Brain : a journal of neurology*. 2013; **136**: 859-71.
44. Lee GJ, Lu PH, Hua X, et al. Depressive symptoms in mild cognitive impairment predict greater atrophy in Alzheimer's disease-related regions. *Biological psychiatry*. 2012; **71**: 814-21.
45. Modrego PJ, Ferrandez J. Depression in patients with mild cognitive impairment increases the risk of developing dementia of Alzheimer type: a prospective cohort study. *Archives of neurology*. 2004; **61**: 1290-3.
46. Andrews-Hanna JR, Snyder AZ, Vincent JL, et al. Disruption of large-scale brain systems in advanced aging. *Neuron*. 2007; **56**: 924-35.
47. Shi F, Liu B, Zhou Y, et al. Hippocampal volume and asymmetry in mild cognitive impairment and Alzheimer's disease: Meta-analyses of MRI studies. *Hippocampus*. 2009; **19**: 1055-64.
48. Wang L, Zang Y, He Y, et al. Changes in hippocampal connectivity in the early stages of Alzheimer's disease: evidence from resting state fMRI. *NeuroImage*. 2006; **31**: 496-504.
49. Hahn A, Wadsak W, Windischberger C, et al. Differential modulation of the default mode network via serotonin-1A receptors. *Proceedings of the National Academy of Sciences of the United States of America*. 2012; **109**: 2619-24.
50. Aznar S, Klein AB. Regulating prefrontal cortex activation: an emerging role for the 5-HT(2)A serotonin receptor in the modulation of emotion-based actions? *Molecular neurobiology*. 2013; **48**: 841-53.
51. Roberts JS, Karlawish JH, Uhlmann WR, et al. Mild cognitive impairment in clinical care: a survey of American Academy of Neurology members. *Neurology*. 2010; **75**: 425-31.
52. Power JD, Barnes KA, Snyder AZ, et al. Spurious but systematic correlations in functional connectivity MRI networks arise from subject motion. *NeuroImage*. 2012; **59**: 2142-54.
53. Wang JH, Zuo XN, Gohel S, et al. Graph theoretical analysis of functional brain networks: test-retest evaluation on short- and long-term resting-state functional MRI data. *PloS one*. 2011; **6**: e21976.
54. First MB, Spitzer RL, Gibbon M, et al. Structured Clinical Interview for DSM-1V TR Axis 1 disorders, research version, non-patient edition (SCID-I/NP). Biometrics Research, New York State Psychiatric Institute, 2002.
55. Lawton MP, Brody EM. Assessment of older people: self-maintaining and instrumental activities of daily living. *Gerontologist*. 1969; **9**: 179-86.
56. Wechsler D. *Manual for the Wechsler Memory Scale-Revised*. Psychological Corporation, 1987.
57. Randolph C. Repeatable Battery for the Assessment of Neuropsychological Status. The Psychological Corporation, 1998.
58. Strogatz SH. Exploring complex networks. *Nature*. 2001; **410**: 268-76.
59. He Y, Chen ZJ, Evans AC. Small-world anatomical networks in the human brain revealed by cortical thickness from MRI. *Cerebral cortex*. 2007; **17**: 2407-19.
60. Wang L, Zhu C, He Y, et al. Altered small-world brain functional networks in children with attention-deficit/hyperactivity disorder. *Human brain mapping*. 2009; **30**: 638-49.
61. Liu Y, Liang M, Zhou Y, et al. Disrupted small-world networks in schizophrenia. *Brain : a journal of neurology*. 2008; **131**: 945-61.

62. He Y, Wang J, Wang L, et al. Uncovering intrinsic modular organization of spontaneous brain activity in humans. *PloS one*. 2009; **4**: e5226.
63. Latora V, Marchiori M. Efficient behavior of small-world networks. *Physical review letters*. 2001; **87**: 198701.
64. Freeman LC. A set of measures of centrality based on betweenness. *Sociometry*. 1977; **40**: 35-41.

2. Supplementary Tables

Table S1. Significant *p*-values of the ANCOVA comparisons of the small-world measurements among the CN, LLD, aMCI, and aMCI-LLD groups

Global Efficiency	Local Efficiency	Path Length	Clustering Coefficient	Sigma
NS	NS	NS	NS	NS
NS	NS	NS	NS	NS
NS	NS	NS	NS	NS
NS	NS	NS	NS	NS
0.0460	NS	0.0453	NS	NS
0.0446	NS	0.0446	NS	NS
0.0428	NS	0.0395	NS	NS
0.0429	NS	0.0473	NS	NS
0.0371	NS	0.0431	NS	NS
0.0414	0.0416	0.0489	NS	NS
0.0296	0.0338	0.0300	NS	NS
0.0219	0.0206	0.0210	NS	NS
0.0142	0.0204	0.0166	NS	NS
0.0127	0.0160	0.0132	NS	NS
0.0161	0.0141	0.0125	NS	NS
0.0166	0.0109	0.0127	NS	NS
0.0146	0.0122	0.0062	NS	NS
0.0168	0.0152	0.0039	NS	NS
0.0131	0.0171	0.0043	NS	0.0324

Note: Only significant *p*-values ($p < 0.05$) are presented.
NS: not statistically significant.

Table S2. Normalized nodal betweenness centrality

Regions	Side	Coordinates (x, y, z)	Normalized Betweenness Centrality			
			CN	LLD	aMCI	aMCI-LLD
PCC-rostral	R	(3, 49, 13)	1.643	1.611	1.443	1.696
VMPFC	L	(-9, -54, 3)	1.428			
dPCC	R	(2, 35, 31)			1.363	1.463
IFG/insula	R	(35, -20, 0)	1.459	1.478		
dACC	R	(1, -15, 44)				1.478
MCC	R	(0, 15, 47)		1.633	1.426	1.435
Insula	L	(-49, -8, -1)		1.706		1.703
Insula	R	(51, -8, -2)		1.478		
Insula	L	(-36, -10, 1)	1.586		1.510	
STG	L	(-65, 33, 20)		1.548		
STG	L	(-58, 16, 7)			1.360	1.540
STG	R	(60, 25, 14)		1.407		
IFG/insula	L	(-36, -22, 3)	1.425			1.492
TPJ	L	(-54, 43, 22)		1.455		
TPJ	R	(55, 40, 14)			1.436	
IPC	L	(-52, 59, 36)			1.445	
Cuneus	L	(-6, 72, 24)	1.416		1.363	
dACC	L	(-5, -23, 37)				1.667
ParaCG	L	(-3, 17, 58)				1.441
PreCG	R	(16, 5, 71)			1.387	

Abbreviations: CN, cognitively normal; LLD, late-life depression; aMCI, amnestic mild cognitive impairment; aMCI-LLD, late-life depression comorbid with amnestic mild cognitive impairment; PCC: posterior cingulate cortex, VMPFC: ventromedial prefrontal cortex, dPCC: dorsal PCC, IFG: inferior frontal gyrus, dACC: dorsal anterior cingulate cortex, MCC: middle cingulate cortex, STG: superior temporal gyrus, TPJ: temporoparietal junction, IPC: inferior parietal cortex, dACC: dorsal anterior cingulate cortex, ParaCG: paracentral gyrus; PreCG: precentral gyrus.

Note: The right rostral posterior cingulate cortex (PCC-rostral) was the only region presented as a hub in all four groups; VMPFC represented a hub only in CN group, and MCC was a hub for all patient groups.

3. Supplementary Figures

Figure S1. Anatomical node representation showing altered nodal efficiency. Gray circles represent uncorrected significant for $p < 0.01$ and black circles represent FDR corrected significant level for $q < 0.05$ and $p < 0.001$.

Abbreviations: CN, cognitively normal; LLD, late-life depression; aMCI, amnestic mild cognitive impairment; aMCI-LLD, late-life depression comorbid with amnestic mild cognitive impairment; dACC: dorsal anterior cingulate cortex, VMPFC: ventromedial prefrontal cortex, MTG: middle temporal gyrus, TP: temporal pole, MCC: middle cingulate cortex, PreCG: precentral gyrus, SFG: superior frontal gyrus, SPC: superior parietal cortex, Precu: precuneus.

Figure S2. Network hub anatomical organization of all four participant groups calculated as the normalized betweenness centrality larger than two standard deviations above the mean.

Abbreviations: CN, cognitively normal; LLD, late-life depression; aMCI, amnestic mild cognitive impairment; aMCI-LLD, late-life depression comorbid with amnestic mild cognitive impairment; PCC: posterior cingulate gyrus, VMPFC: ventral medial prefrontal cortex, dPCC: dorsal PCC, IFG: inferior frontal gyrus, dACC: dorsal anterior cingulate cortex, MCC: middle cingulate cortex, STG: superior temporal gyrus, TPJ: temporoparietal junction, IPC: inferior parietal cortex, PreCG: precentral gyrus.

Figure S3. Normalized betweenness centrality for the participant groups. Abbreviations: CN, cognitively normal; LLD, late-life depression; aMCI, amnestic mild cognitive impairment; aMCI-LLD, late-life depression comorbid with amnestic mild cognitive impairment.

Figure S1

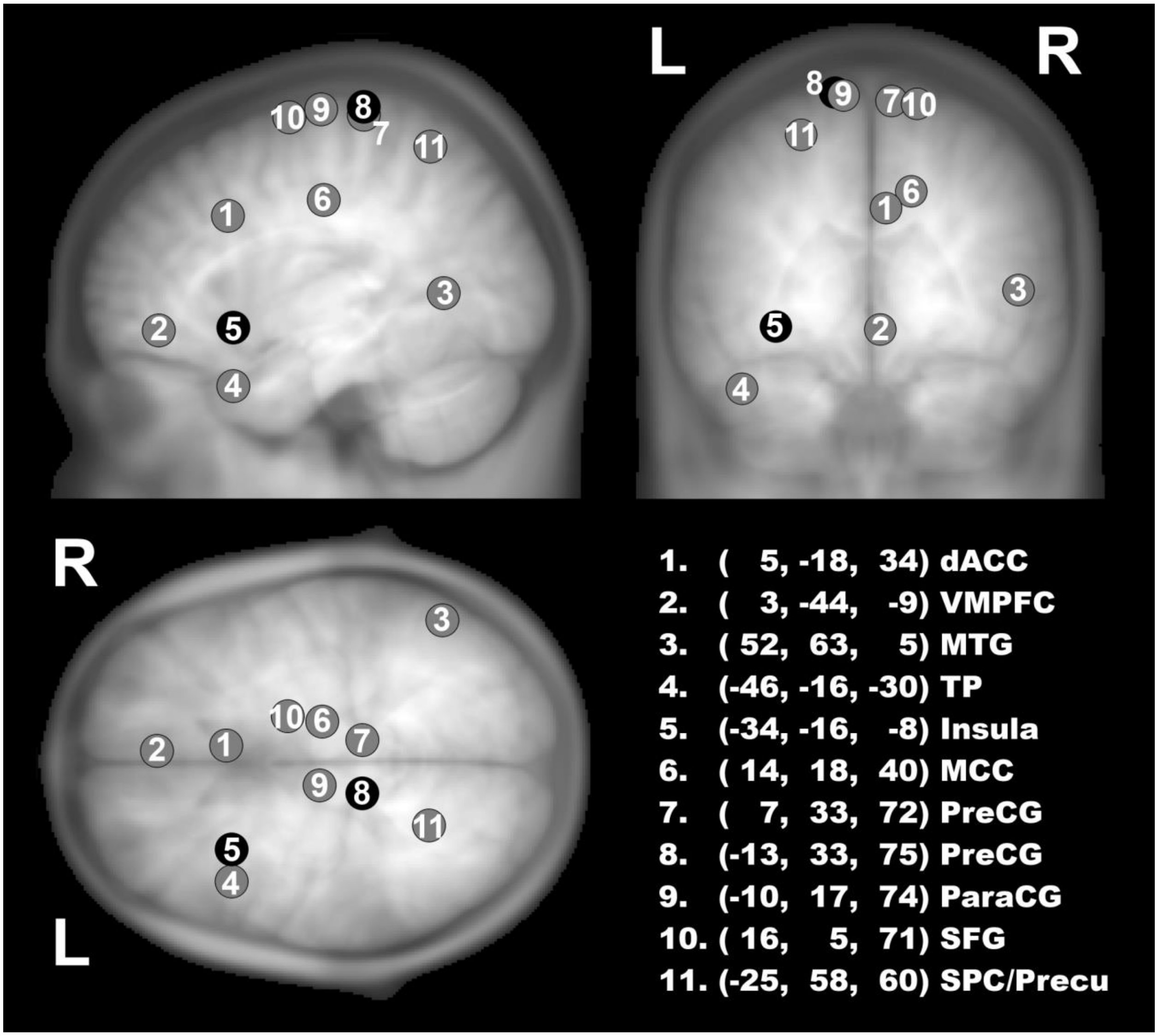
L
R
8
9
7
10
11
6
1
3
5
2
4
R
L
1. (5, -18, 34) dACC
2. (3, -44, -9) VMPFC
3. (52, 63, 5) MTG
4. (-46, -16, -30) TP
5. (-34, -16, -8) Insula
6. (14, 18, 40) MCC
7. (7, 33, 72) PreCG
8. (-13, 33, 75) PreCG
9. (-10, 17, 74) ParaCG
10. (16, 5, 71) SFG
11. (-25, 58, 60) SPC/Precu

Figure S2.

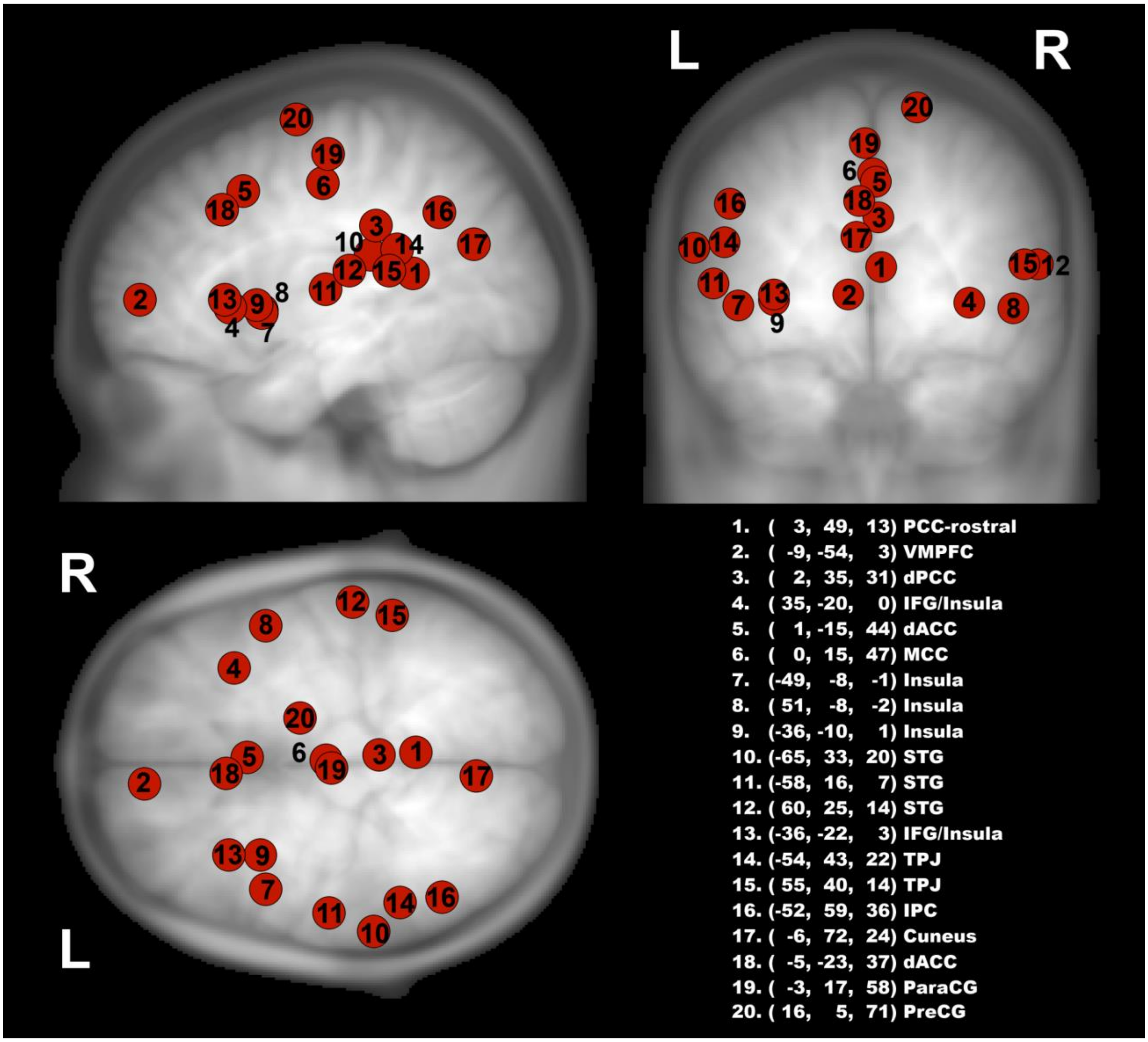
L
R
R
L
1. (3, 49, 13) PCC-rostral
2. (-9, -54, 3) VMPFC
3. (2, 35, 31) dPCC
4. (35, -20, 0) IFG/Insula
5. (1, -15, 44) dACC
6. (0, 15, 47) MCC
7. (-49, -8, -1) Insula
8. (51, -8, -2) Insula
9. (-36, -10, 1) Insula
10. (-65, 33, 20) STG
11. (-58, 16, 7) STG
12. (60, 25, 14) STG
13. (-36, -22, 3) IFG/Insula
14. (-54, 43, 22) TPJ
15. (55, 40, 14) TPJ
16. (-52, 59, 36) IPC
17. (-6, 72, 24) Cuneus
18. (-5, -23, 37) dACC
19. (-3, 17, 58) ParaCG
20. (16, 5, 71) PreCG

Figure S3.

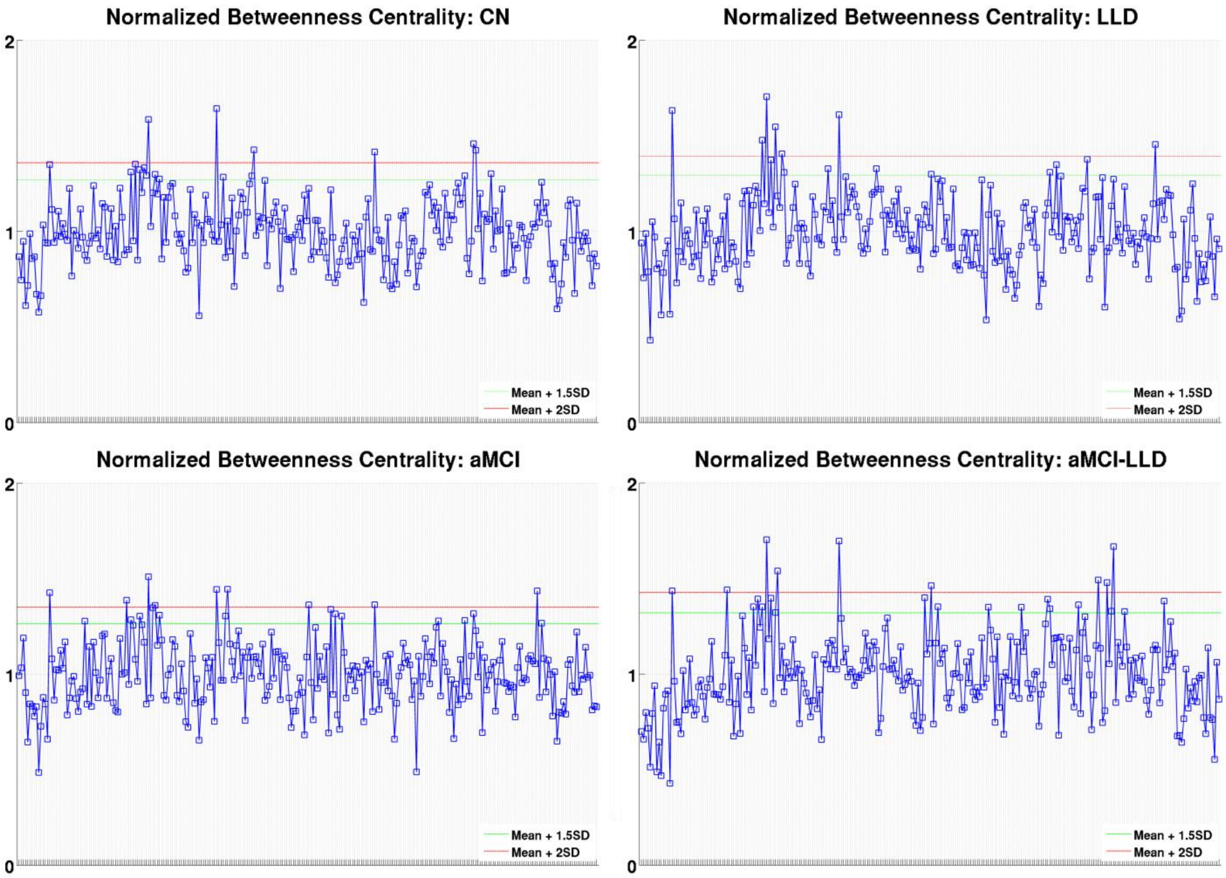
Normalized Betweenness Centrality: CN
Normalized Betweenness Centrality: LLD
Normalized Betweenness Centrality: aMCI
Normalized Betweenness Centrality: aMCI-LLD
2
1
0
Mean + 1.5SD
Mean + 2SD